Proceedings for the 5th International Fire Behavior and Fuels Conference
April 11-15, 2016, Portland, Oregon, USA
Published by the International Association of Wildland Fire, Missoula, Montana, USA

Assimilation of Satellite Active Fires Detection Into a Coupled Weather-Fire Model

Jan Mandel*
University of Colorado Denver, Denver, Colorado, USA, jan.mandel@gmail.com

Aimé Fournier
University of Colorado Denver, Denver, Colorado, USA, aime.fournier@ucdenver.edu

Mary Ann Jenkins
York University, Toronto, Ontario, Canada, maj@yorku.ca

Adam K. Kochanski
University of Utah, Salt Lake City, Utah, USA, adam.kochanski@utah.edu

Sher Schranz
Colorado State University and NOAA, Boulder, Colorado, USA, sher.schranz@noaa.gov

Martin Vejmelka
AVAST Software s.r.o., Prague, Czech Republic, vejmelkam@gmail.com

Introduction

Active fire detection products from the VIIRS and MODIS instruments on polar-orbiting satellites provide planet-wide fire detection at resolutions from 375 m to 1.1 km every 6 or 12 hours. Because the data products are continuously available online, they present an attractive data source for automated fire behavior simulations and forecasts. Active fire detection was used to initialize simulations previously (Coen and Schroeder, 2013). However, the scale of fire simulation is typically finer (30m-200m) than the scale of the satellite fire detection, there are false positive and false negative detection errors as well as geolocation errors, and there is no detection under clouds (Hawbaker *et al.*, 2008, Schroeder *et al.,* 2014). For these reasons, we believe that satellite detection should be used in fire simulation in a statistical sense only, rather than as a direct data input.

In this contribution, we study the use of Level 2 MODIS and VIIRS Active Fires products in a statistical framework similar to that in Mandel *et al.* (2014b), which used Level 3 data. Level 3 fire detections are already fused from different satellite sources over a single area, which makes their use more convenient, but the distinction between not burning and no information available is lost, which limits their use in data assimilation, and they are not recommended for science use (Giglio, 2015). Level 2 data are grid based, and the data values on every node of the grid specify if no information is available, if the sensor detected water or ground without fire, or if a fire was detected. The confidence of a fire detection is given as one of three levels (low, nominal, high). Unfortunately, no confidence level is available for water or

* Department of Mathematical and Statistical Sciences, University of Colorado Denver, Denver, CO 80217-3364.

ground detection with no fire. Level 2 active fires data come as granules, which are areas under the satellite path over several minutes of flight. The granules are presented on a rectangular grid, with a uniform longitude-latitude grid spacing (Fig. 1). A granule may or may not contain the area of interest, or it may intersect it only partially (Fig. 2), and there can be occasional detection artifacts (Fig. 3).

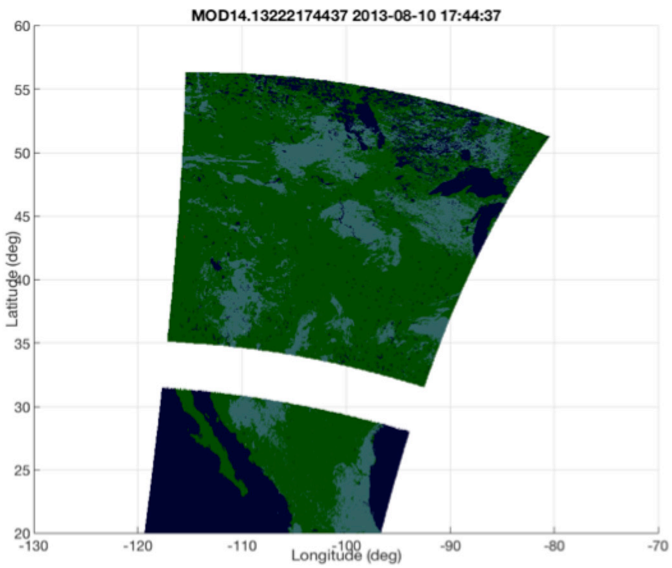

Figure 1. A MODIS Active Fires detection granule in false colors: blue=water, green = groud, grey= cloud, red = fire, white = no data. The fire pixels are too small to see at this scale.

Methods

Model

We are using the coupled atmosphere-fire model WRF-SFIRE (Mandel *et al*., 2009; 2011; 2014a), which combines the community WRF model (Skamarock *et al*., 2008) with the fire spread implemented by the level set method. A limited version of the software from 2010 is contained in WRF release as WRF-Fire (Coen *et al*., 2013). The fire state in the WRF-

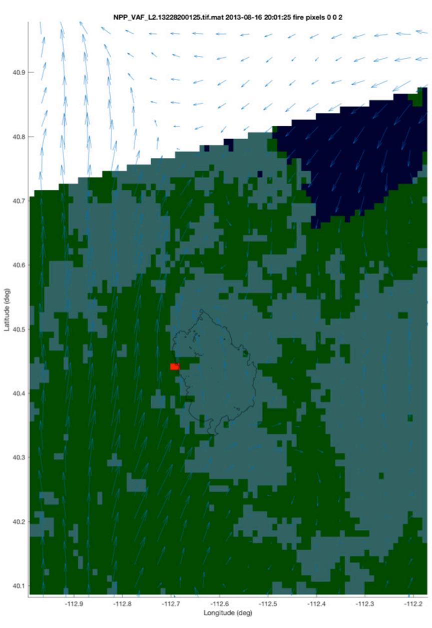

Figure 2. VIIRS Active Fires detection in false colors same as in Fig. 1, shown with the fire perimeter and ground wind field from WRF-SFIRE simulation of 2013 Patch Springs fire, UT. The granule only partially intersects the area of interest, and there is a significant cloud cover.

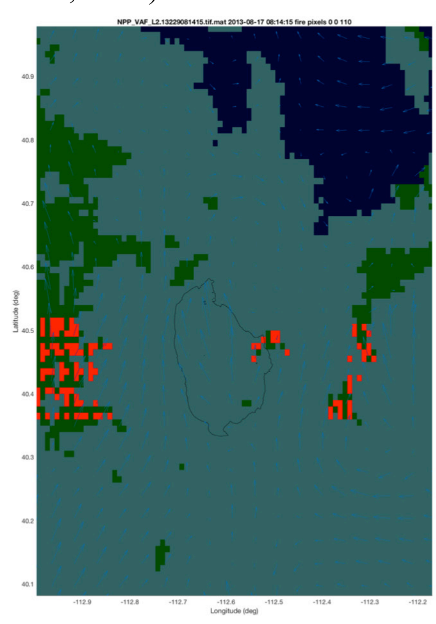

Figure 3. VIIRS Active Fires detection in false colors and with simulated fire perimeter and ground wind field as in Fig. 2. The horizontal band of false detections is a data artifact. Note almost complete cloud cover over the fire. The validity of the detections on the edge of the fire is unclear.

SFIRE model was encoded as fire arrival time T, with a value given at every node in a grid on the surface of the Earth. The fire arrival time can be modified by data assimilation and inserted back into the model. The atmosphere model can be then restarted from a checkpoint at a time in the past and driven by fire heat fluxes generated by the modified fire arrival time, which allows the proper atmospheric circulation to develop. At the time of the observation, the fire model and the two-way coupling with the atmosphere takes over again. This technique was originally developed in the context of ignition from a given fire perimeter (Mandel *et al.*, 2012; Kochanski *et al.*, 2016).

Data assimilation

The satellite data are assimilated in the fire arrival time using the Maximum Aposteriori Probability (MAP) estimator (e.g., Stuart, 2010) from Bayesian statistics. Given forecast fire arrival time $T^{\mathrm{f}} = T^{\mathrm{f}}(x,y)$ on the simulation domain, we maximize the aposteriori probability density

$$p^{\mathrm{a}}\left(T\right) = \mathrm{const}\; e^{\sum_G \sum_{(x,y)\in G} c_G(x,y) f_{G,x,y}(T-t_G,x,y)} e^{-\frac{\alpha}{2}\left\|T-T^{\mathrm{f}}\right\|_A^2} \to \max_T,$$

which is equivalent to the penalized optimization problem,

$$-\sum_G \sum_{(x,y)\in G} c_G(x,y) f_{G,x,y}(T-t_G,x,y) + \frac{\alpha}{2}\left\|T-T^{\mathrm{f}}\right\|_A^2 \to \min_T.$$

Here, the first sum is over the assimilated granules G, the second sum is over the grid nodes (x,y) in the intersection of the granule G and the simulation domain, and $c_G(x,y)$ is the confidence level of the granule G data at the location (x,y). When no data are available for the location, e.g., because of a cloud, $c_G(x,y)$ is taken to be zero. The quantity $f_{G,x,y}$ is the log likelihood – the natural logarithm of the conditional probability of the observed value (fire detection or non-detection) given the fire arrival time. The probabilities of fire detection in MODIS and VIIRS pixels are available from statistical assessment of active fires detection by comparison with high-resolution limited-area satellite imagery (Schroeder *et al.*, 2008, 2014) and logistic regression, which leads to a data likelihood similar as in Mandel *et al.* (2014b). In the second term, $\alpha > 0$ is the penalty parameter, and the squared norm in the penalty term is defined as

$$\left\|u\right\|_A^2 \approx \int u\left(-\frac{\partial^2}{\partial x^2}-\frac{\partial^2}{\partial y^2}\right)^a u\,dx\,dy,\; a>1,$$

where the fractional power of the Laplace operator is implemented efficiently by Fast Fourier Transform (FFT). The penalty term results in a preference for smooth changes in the fire arrival time T, and it prevents overfitting the estimate to the uncertain and sparse data. The minimization is done subject to the constraint that the fire arrival time is fixed at the point of ignition, by a preconditioned gradient descent with a line search. One or two iterations are sufficient for acceptable results. See Mandel *et al.* (2014b) for further details of this computational method.

Results

The method was tested on the 2013 Patch Springs fire. The simulation was done at a relatively coarse resolution, 200m fire grid and 4000m atmospheric grid, thus mimicking the situation when the simulation needs to run much faster than real time. The 9 days simulation period started at 00:00 Aug11, 2013 GMT, and the fire was ignited 2 hours into the simulation. The forecast state, i.e., the result of the simulation, is shown in Fig. 4. Fig. 5 shows the analysis state, i.e., with the detections assimilated. In both Fig. 4 and Fig. 5, the available fire detections from the MODIS and the VIIRS instruments are shown for comparison. Brighter squares have higher confidence of detection and the time-space fire arrival time surface is drawn transparent, so detections inside the fire are (more faintly) visible. The horizontal levels of the clusters of fire pixels correspond to the satellite overflight times. In Fig. 4, the forecast shows many detections outside of the fire, indicating the need for an adjustment of the model state. In Fig. 5, most, but not all, detections are inside the fire in the analysis state. The figures suggest that the fire may have started in a slightly different location (about 0.03 degrees South and West) and at least a day earlier than in the forecast. A relatively large error in the ignition is plausible, because the simulation was started from inexact ignition data, namely a verbal description of the estimated ignition point and time in the incident report.

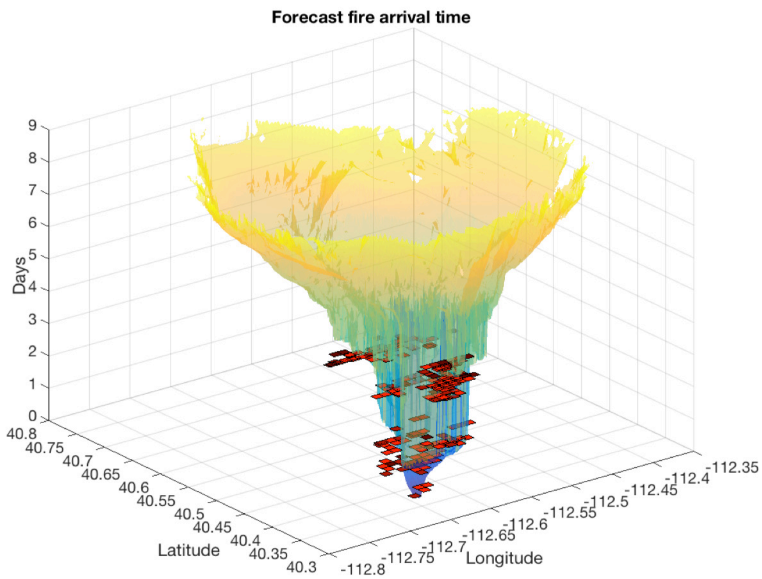

Figure 4. Fire arrival time before the assimilation (called forecast in data assimilation), with MODIS and VIIRS Active Fires detections.

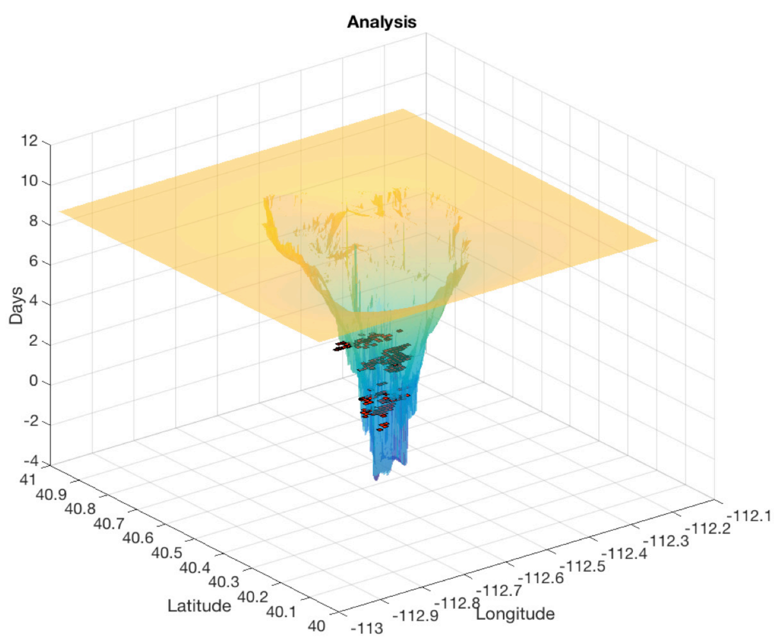

Figure 5. Analysis fire arrival time, with the MODIS and VIIRS Active Fires detections assimilated.

Conclusion and future work

We have demonstrated a data assimilation technique, which can modify the state of the fire spread model from Level 2 Active Fires MODIS and VIIRS data. The likelihood of detection depends on the brightness in the whole MODIS or VIIRS pixel, as used in the statistical assessments of the active fires detection (Morisette *et al.*, 2005; Schroeder *et al*., 2008, 2014). This approach follows the properties of the hardware (Cao *et al.*, 2014) and the software (Schroeder *et al.*, 2014) stack, in particular the discrete nature of the rows of the CCD sensors in the imager hardware, which effectively integrate the signal over their pixels. However, while the actual scanning is aligned with the flight path, the pixels in Level 2 products are already processed into a rectangular longitude-latitude mesh. In particular, they are distinct from the original integration of the signal by the sensor. In this paper, we interpolate the Level 2 fire detection data further onto our 200m computational mesh, which is then used to compute the data likelihood. Even if reasonable results were obtained, it might be more consistent with the statistical properties of the active fires detection to integrate the fire effect over larger areas comparable in size to the Level 2 product pixels, and in particular the instrument resolution, and use that integrated effect to compute the data likelihood. More accurate, physically and statistically based data likelihood should be also developed. Next, our current method assumes a given fixed location of the ignition point. Work on estimating the ignition point from uncertain and sparse detections is in progress (James Haley) and it should become a part of the optimization process. These techniques will eventually allow a completely autonomous simulation of a wildland fire with no other fire data than satellite sensing. Finally, incident data should be brought in to determine when a change in fire behavior is due to firefighting efforts rather than model or data inaccuracy. With the increasing role of Information Technology (IT) in fire management, this may become possible in near future.

Acknowledgements

This research was partially supported by the NSF grant DMS1216481 and NASA grant NNX13AH59G. This work partially utilized the Colibri cluster at the Center for Computational Mathematics, University of Colorado Denver, supported by NSF grant CNS-0958354. We would like to thank Brad Quale and David Hayes from USDA Forest Service Remote Sensing Applications Center (RSAC) for providing the Level 2 Active Fires data processed into a convenient GeoTIFF format. We would also like to thank the participants in the Data Assimilation Seminar at the Department of Mathematical and Statistical Sciences, University of Colorado Denver, in particular Loren Cobb, Dmitry Ostrovsky, James Haley, Tian Yu Yen, and Ivan Kasanický, for bearing with multiple presentations of versions of this project and useful discussions.

References

Cao C, Luccia FJD, Xiong X, Wolfe R, Weng, F (2014) Early on-orbit performance of the Visible Infrared Imaging Radiometer Suite onboard the Suomi National Polar-Orbiting Partnership (S-NPP) satellite. *IEEE Transactions on Geoscience and Remote Sensing* **52**, 1142–1156, doi:10.1109/TGRS.2013.2247768.

Coen JL, Cameron M, Michalakes J, Patton EG, Riggan PJ, Yedinak, K (2013) WRF-Fire: Coupled weather-wildland fire modeling with the Weather Research and Forecasting model.

Journal of Applied Meteorology and Climatology **52**, 16–38, doi:10.1175/JAMC-D-12-023.1.

Coen JL, Schroeder W (2013) Use of spatially refined satellite remote sensing fire detection data to initialize and evaluate coupled weather-wildfire growth model simulations. *Geophysical Research Letters* **40**, 1–6, doi:10.1002/2013GL057868.

Giglio L (2015) MODIS collection 6 active fire product user's guide version 2.6. Department of Geographical Sciences, University of Maryland, available at http://modis-fire.umd.edu/files/MODIS_C6_Fire_User_ Guide_A.pdf, accessed March 2015.

Hawbaker TJ, Radeloff VC, Syphard AD, Zhu Z, Stewart SI (2008) Detection rates of the MODIS active fire product in the United States, *Remote Sensing of Environment* **112**, 2656–2664. doi:10.1016/j.rse.2007.12.008

Kochanski AK, Jenkins MA, Kondratenko VY, Schranz S, Vejmelka M, Clements CB, Davis B (2016) Ignition from fire perimeter and assimilation into a coupled fire-atmosphere model. In Proceedings for the 5th International Fire Behavior and Fuels Conference April 11-15, 2016, Portland, Oregon, USA.

Mandel J, Beezley JD, Coen JL, Kim M (2009) Data assimilation for wildland fires: Ensemble Kalman filters in coupled atmosphere-surface models. *IEEE Control Systems Magazine* **29**, 47–65, doi:10.1109/MCS.2009.932224.

Mandel J, Beezley JD, Kochanski AK (2011) Coupled atmosphere-wildland fire modeling with WRF 3.3 and SFIRE 2011. *Geoscientific Model Development* **4**, 591–610, doi:10.5194/gmd-4-591-2011.

Mandel J, Beezley JD, Kochanski AK, Kondratenko VY, Kim M (2012) Assimilation of perimeter data and coupling with fuel moisture in a wildland fire – atmosphere DDDAS. *Procedia Computer Science* **9**, 1100–1109, doi:10.1016/j.procs.2012.04.119.

Mandel J, Amram S, Beezley JD, Kelman G, Kochanski AK, Kondratenko VY, Lynn BH, Regev B, Vejmelka M (2014a): Recent advances and applications of WRF-SFIRE. *Natural Hazards and Earth System Science* **14**, 2829–2845, doi:10.5194/nhess-14-2829-2014.

Mandel J, Kochanski AK, Vejmelka M, Beezley JD (2014b) Data assimilation of satellite fire detection in coupled atmosphere-fire simulations by WRF-SFIRE. In Advances in Forest Fire Research (Ed DX Viegas), pp. 716–724 (Coimbra University Press)

Morisette JT, Giglio L, Csiszar I, Setzer A, Schroeder W, Morton D, Justice CO (2005) Validation of MODIS active fire detection products derived from two algorithms. *Earth Interactions* **9**, 1–25, doi:10.1175/EI141.1.

Schroeder W, Prins E, Giglio L, Csiszar I, Schmidt C, Morisette J, Morton D (2008) Validation of GOES and MODIS active fire detection products using ASTER and ETM+ data. *Remote Sensing of Environment* **112**, 2711–2726, doi:10.1016/j.rse.2008.01.005.

Schroeder W, Oliva P, Giglio L, Csiszar IA (2014) The New VIIRS 375 m active fire detection data product: Algorithm description and initial assessment. *Remote Sensing of Environment* **143**, 85– 96, doi:10.1016/j.rse.2013.12.008.

Skamarock WC, Klemp JB, Dudhia J, Gill DO, Barker DM, Duda MG, Huang XY, Wang W, Powers JG (2008) A description of the Advanced Research WRF version 3. NCAR Technical Note 475, http://www.mmm.ucar.edu/wrf/users/docs/arw_v3.pdf, retrieved December 2011.

Stuart AM (2010) Inverse problems: a Bayesian perspective. *Acta Numerica* **19**, 451– 559, doi:10.1017/S0962492910000061.